

## Hydrogen Clusters that Remain Fluid at Low Temperature

Kirill Kuyanov-Prozument\* and Andrey F. Vilesov

*Department of Chemistry, University of Southern California, Los Angeles, California 90089, USA*  
(Received 7 March 2008; revised manuscript received 3 July 2008; published 13 November 2008)

Superfluidity of hydrogen, predicted three decades ago, continues to elude experimental observation, due to the high freezing temperature of  $H_2$  at  $T = 13.8$  K. Here, large *para*- $H_2$  clusters are obtained in a cryogenic pulsed free jet expansion and are studied via nonlinear Raman spectroscopy. Clusters formed from neat  $pH_2$  are solid as evidenced by the characteristic splitting of the rotational  $S_0(0)$  line. However, clusters formed of highly diluted  $pH_2$  ( $\leq 1\%$ ) in He have a single  $S_0(0)$  line and remain liquid at the estimated superfluid transition temperature of  $T = 1-2$  K.

DOI: 10.1103/PhysRevLett.101.205301

PACS numbers: 67.10.-j, 67.25.dw, 67.63.-r, 78.30.-j

Study of superfluidity in He isotopes [1] and, more recently, in extremely rarified clouds of alkali atoms [2], has advanced our knowledge of the many body quantum phenomena and has provided one of the very few examples of a macroscopic wave function. At sufficiently low temperatures, both trapped alkali atoms and liquid  $^4He$  are 100% superfluid. However, the former is a nearly pure Bose-Einstein condensate (BEC), whereas the latter has a small fraction of BEC ( $\sim 10\%$ ). While it is generally agreed that there is a close association between Bose-Einstein condensation and superfluidity, the exact relation has yet to be established [3]. Accordingly, there is a strong motivation to discover new superfluid substances. Presently, *parahydrogen* ( $pH_2$ ) remains the only feasible candidate [4]: it has a calculated superfluid transition temperature at  $\approx 1.1$  K in the bulk [5],  $\approx 2$  K in small clusters [6], and should have an even smaller Bose-condensed fraction than  $^4He$  [7]. Hydrogen may also constitute a new class of *molecular superfluids* that are characterized by anisotropic interaction and rotational angular momentum of the particles.

Freezing of hydrogen at 13.8 K is the primary experimental obstacle. Although the rate of freezing is predicted to be very low at  $T \leq 3$  K [8], numerous attempts at supercooling liquid hydrogen in macroscopic droplets [9], clusters [10,11], porous media [12], or in the bulk [13] have proven unsuccessful. In this work, we have adopted a different approach which includes assembling large clusters from  $pH_2$  molecules at low temperatures by free jet expansion of  $pH_2$  gas seeded in He. Using Raman spectroscopy we show that such clusters remain liquid at  $T = 1-2$  K, advancing experiments into the temperature range of the predicted superfluid transition.

The hydrogen clusters are obtained in a pulsed free jet expansion [14] of either a liquid or a cold gas mixture of  $pH_2$  in He at a stagnation pressure of  $P_0 = 20$  bar. The  $pH_2$  is produced by catalytic conversion of liquid  $H_2$  and contains less than 0.1% of *ortho*- $H_2$  ( $oH_2$ ). Similar to  $^4He$  atoms,  $pH_2$  molecules are spinless bosons ( $I = 0$ ) and at low temperature reside in the ground rotational state  $J = 0$ , which makes  $pH_2$  the prime candidate for observation of superfluidity. Higher degeneracy and stronger intermolec-

ular interaction in  $oH_2$  ( $I = 1, J = 1$ ) depress its transition temperature [4] and cause faster freezing [9].

The spectra of the clusters are obtained via coherent anti-Stokes Raman scattering (CARS) [15]. In this nonlinear spectroscopic technique, two 532 nm pump beams from a Nd:YAG laser and a Stokes beam from a dye laser are focused onto the same point in the path of the gas expansion. When the frequency difference of the pump and Stokes laser beams matches the vibrational or rotational frequency of the  $pH_2$  molecules, an anti-Stokes signal is generated, which is detected by a photomultiplier.

The vibrational frequency of the hydrogen molecules decreases by about  $10\text{ cm}^{-1}$  upon condensation and thus is a useful monitor of cluster formation in the jet. Figure 1 is an example of a vibrational CARS spectrum obtained upon the expansion of a gas mixture consisting of 0.5%  $pH_2$  in helium. A strong peak at  $4150.5\text{ cm}^{-1}$  and a weak, narrow peak at  $4161.13\text{ cm}^{-1}$  are assigned to the  $Q_1(0)$  ( $\nu' = 1, J' = 0$ )  $\leftarrow$  ( $\nu'' = 0, J'' = 0$ ) lines of  $pH_2$  molecules in the clusters and in the gas phase, respectively. Upon magnification, an additional broad ( $\delta\nu \approx 3\text{ cm}^{-1}$ ) feature centered at about  $4156.5\text{ cm}^{-1}$  is seen in the spectrum. We attributed the broad band to the molecules on the surface of

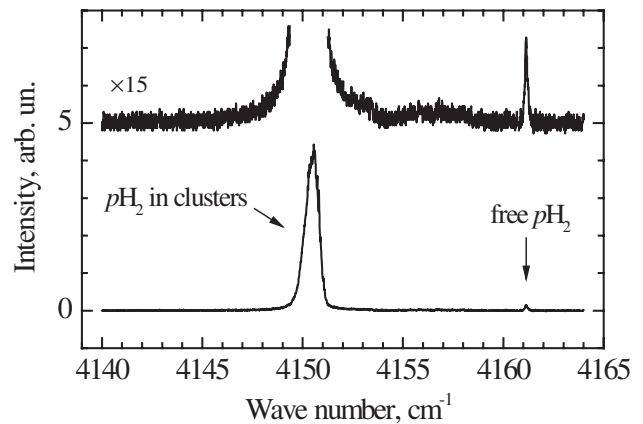


FIG. 1. Vibrational CARS spectrum obtained upon expansion of 0.5%  $pH_2$  in He at  $T_0 = 17$  K. The magnified trace is offset for clarity.

the clusters. Because of the incomplete coordination, the vibrational frequency of the surface molecules is approximately halfway between that in the interior of the cluster and that in the gas phase. The large width of the surface band must be related to a broader distribution of intermolecular distances at the surface as compared to the interior. The intensity of the surface band allows estimation of the size of the clusters, as is discussed later.

Vibrational spectra such as in Fig. 1 were recorded for clusters of different size and temperature, which were obtained by varying the fraction,  $X$ , of  $p\text{H}_2$  in the expanding He gas. For each  $X$  the cluster's signal was observed within a certain range of the nozzle temperatures  $\Delta T_0 \approx 15$  K, which is determined by condensation of  $p\text{H}_2$  inside the nozzle assembly at low  $T_0$  and by inefficient clustering at high  $T_0$ . Mass spectrometric measurements about 1 m downstream from the nozzle revealed the appearance of the mass  $M = 8 u$  peak at  $T_0 < 19$  K, which indicates the formation of He droplets. At these conditions, such as in Fig. 1, the  $p\text{H}_2$  clusters are likely encapsulated in the He droplets. Nevertheless, the frequencies of the  $Q_1(0)$  line remained constant at different  $T_0$  with or without He droplets. In order to maximize the signal, the spectra shown in this work have been obtained at short distance from the nozzle ( $L = 5$  mm).

The frequency of the  $Q_1(0)$  line is known to be lower in solid than in liquid [16,17], and can therefore be used as a probe of the state of the clusters. Figure 2 shows the frequency of the  $Q_1(0)$  line in clusters vs  $X$ , with  $X = 100\%$  corresponding to an expansion of neat liquid  $p\text{H}_2$ . At  $X = 2\% - 100\%$  the frequency of the  $Q_1(0)$  line in those clusters is the same as in the bulk solid [16], within error limits of about  $\pm 0.2$   $\text{cm}^{-1}$ . Figure 2 shows that upon decrease of  $X$  from 2% to 0.5%, the frequency of the  $Q_1(0)$  line increases abruptly by about  $1$   $\text{cm}^{-1}$ , towards the frequency in liquid  $p\text{H}_2$ .

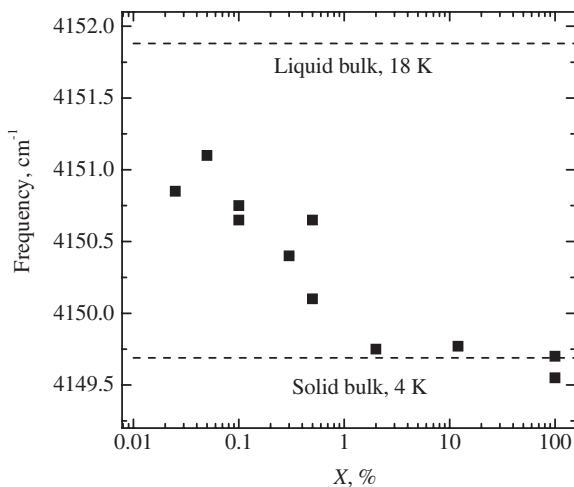


FIG. 2. Frequency of the  $Q_1(0)$  line in clusters vs fraction of the  $p\text{H}_2$  molecules in the expanding He gas— $X$ . Horizontal dashed lines show the  $Q_1(0)$  frequencies in solid  $p\text{H}_2$  at 4 K [16] and in liquid  $p\text{H}_2$  at 18 K [17].

In order to determine the physical state of the clusters, we then measured the spectra of the rotational  $S_0(0)$  line ( $\nu' = 0, J' = 2$ )  $\leftarrow$  ( $\nu'' = 0, J'' = 0$ ) at different  $X$ , which are shown in Fig. 3. A sharp  $S_0(0)$  line in free  $p\text{H}_2$  molecules at  $354.38$   $\text{cm}^{-1}$  is labeled by the dotted line in panels (a)–(d). Spectra of clusters formed at  $X = 100\%$  and  $10\%$  in Figs. 3(a) and 3(b) show split  $S_0(0)$  lines, which is a clear indication of the solid state of the clusters. In the solid, the degeneracy of the  $J = 2$  rotational state is lifted by electric quadrupole-quadrupole and crystal field type intermolecular interactions. The resulting Raman spectrum is a well-defined triplet and doublet in the hcp and fcc lattices [17–19], respectively, as shown in Figs. 3(a) and 3(b) by vertical bars. In the bulk solid the hcp phase prevails [17]. However, the waveform of the cluster's spectrum resembles that in fcc, but has some additional features, such as a split lower frequency line. Similar spectra have been observed in irregular  $p\text{H}_2$  or *ortho*- $\text{D}_2$  solids, obtained via low temperature surface deposition [18] or upon application of pressure to solid samples [20].

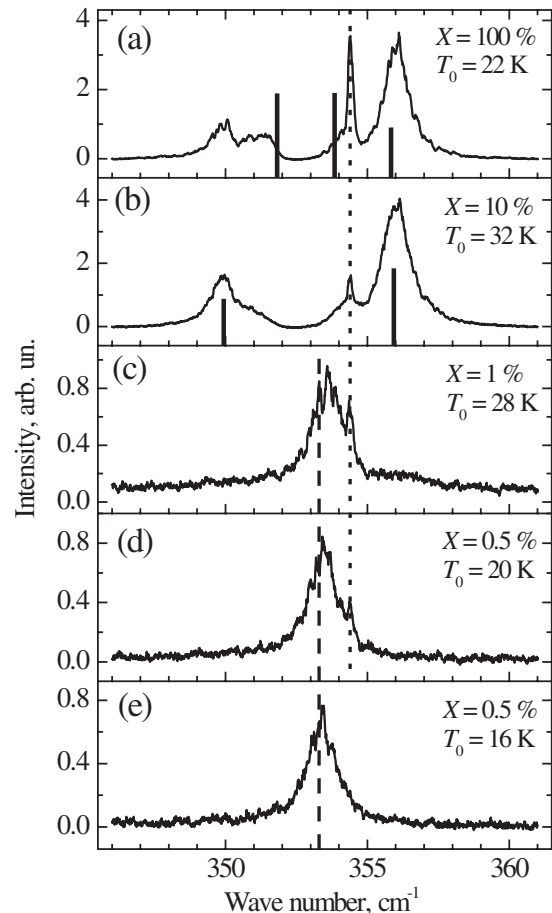


FIG. 3. Rotational CARS spectra of  $p\text{H}_2$  clusters obtained at different  $X$  and  $T_0$  as indicated in each panel. The frequencies of the  $S_0(0)$  lines in gaseous and in liquid  $p\text{H}_2$  at 18 K are shown by vertical dotted and dashed lines, respectively [17]. The split  $S_0(0)$  lines in hcp and in fcc solid  $p\text{H}_2$  are shown by vertical bars in panels (a) and (b), respectively [17,18].

The spectra obtained at  $X = 1\%$  and  $0.5\%$  in Figs. 3(c)–3(e), however, have a single  $S_0(0)$  line similar to that in bulk liquid  $p\text{H}_2$  [17]. The single  $S_0(0)$  line in Figs. 3(c)–3(e) is strong evidence of the liquid state of the clusters obtained at  $X \leq 1\%$ . The absence of splitting and the rather small width of the  $S_0(0)$  line must be a result of the averaging of the anisotropic interaction of a molecule with its nearest neighbors in the liquid and concomitant motional narrowing of the spectrum.

Because of the low nozzle temperature, the  $p\text{H}_2$  clusters in Fig. 3(e) are likely entrained in He droplets. On the other hand, there are no droplets in the beam at higher  $T_0$  in Figs. 3(c) and 3(d). Comparison of the spectra shows that the entrainment in the droplets does not lead to any noticeable change in the shape of the  $S_0(0)$  line in liquid  $p\text{H}_2$  clusters.

We proceed with an estimate of the temperature of the clusters. Because of the large nozzle diameter of  $d_0 = 1$  mm, the observation point at  $L/d_0 = 5$  corresponds to an ongoing supersonic expansion with a high frequency of collisions [21]. Thus, the local temperature of the expanding He gas can be obtained as [21]

$$T = T_0 \times 0.35 \left( \frac{d_0}{L} \right)^{4/3}. \quad (1)$$

The release of the latent energy of condensation of  $p\text{H}_2$  of about 105 K per molecule leads to an increase of the temperature in the beam. Thus the temperatures of the liquid clusters in Figs. 3(c) and 3(d) are about or less than 2.2 and 1.3 K, respectively. Likewise, the temperature of the solid clusters obtained at  $X = 10\%$  in Fig. 3(b) is about 10 K.

At low  $T_0 = 16$  K,  $p\text{H}_2$  clusters in Fig. 3(e) are likely embedded in He droplets, whose temperature is estimated to be less than about 2 K based on the following considerations. The density of the He gas at the observation point  $\rho_g$  can be obtained using the ideal gas expansion results of Ref. [21] to be about  $10^{20}$  atoms/cm<sup>3</sup>. The actual  $\rho_g$  is somewhat lower due to formation of He droplets. Because of the small  $L/d_0$  and large  $\rho_g$  growth of the He droplets is expected to continue at the observation point. Therefore, the system is supersaturated, and the temperatures of both the gas and the droplets must be lower than the temperature of the saturated vapor at  $\rho_g$ , which is about 2 K. Further downstream of the jet the temperature drops due to onset of evaporative cooling and can be as low as  $T = 0.38$  K [22,23] in high vacuum. Thus, the encapsulation can be used to cool  $p\text{H}_2$  clusters well below the predicted superfluid transition temperature at distances far enough from the nozzle.

Finally, clusters in Fig. 3(a) have been obtained by expansion of liquid  $p\text{H}_2$ , which in vacuum breaks up into large clusters. The temperature of the clusters is determined by liquid jet expansion [24] and subsequent evaporative cooling, but is difficult to estimate. It must be lower than 13.8 K to obtain solid clusters, but higher than the 4 K

predicted for  $\text{H}_2$  clusters in vacuum [24]. It is seen that the solid  $p\text{H}_2$  clusters have much higher temperature than the liquid clusters. In an attempt to rationalize this counterintuitive result, we consider the mechanism of freezing of  $\text{H}_2$ .

According to classical theory, the rate of homogeneous nucleation is limited by the creation of a nucleus of some critical size by thermal fluctuations. The rate of classical nucleation in liquid hydrogen increases exponentially upon decrease of temperature, passes through a maximum between 6 and 9 K, and then falls exponentially at lower temperature [9,25]. Upon expansion of the  $p\text{H}_2$  liquid and gas of  $X = 10\%$ , warm liquid clusters are formed. The clusters then cool further downstream from the nozzle, enter the range of high nucleation rate, and freeze. Previously, the freezing of the large clusters obtained in a nozzle expansion of neat  $p\text{H}_2$  gas has been observed in Ref. [11]. In Ref. [9] liquid  $p\text{H}_2$  droplets of about 50  $\mu\text{m}$  diameter have been observed only at temperatures higher than 10.7 K. It follows that cold liquid  $\text{H}_2$  clusters cannot be obtained via supercooling.

The formation of cold liquid clusters in this work is consistent with an alternative mechanism. During the expansion of strongly diluted  $p\text{H}_2$ , the temperature drops rapidly along the expansion path according to Eq. (1), and the growth of the clusters occurs at low temperatures. At  $T \lesssim 3$  K the rate of classical nucleation is negligible and nucleation by quantum tunneling is expected to be the principal mechanism of hydrogen freezing [9,25]. Observation of liquid clusters at  $T \lesssim 2$  K in this work shows that the rate of quantum nucleation must be less than about  $1 \text{ s}^{-1} \text{ molecule}^{-1}$ . Thus at low temperature the clusters grow while staying in the liquid phase, which is facilitated by a very low rate of both quantum and classical nucleation. Other factors which may aid the stability of the liquid in the clusters, as compared to the bulk, are the lower freezing point and slower nucleation rate due to finite size effects [25].

Hydrogen appears to be unique in that its freezing point can be depressed all the way down to  $T = 0$  K upon decrease of the cluster size. Small clusters consisting of less than about  $N = 30$   $p\text{H}_2$  molecules are predicted to have a superfluid transition at  $T \leq 2$  K [6]. The only experimental indication of superfluidity in small  $p\text{H}_2$  clusters came from the infrared spectra of carbonyl sulfide (OCS) molecules with up to 16  $p\text{H}_2$  molecules assembled in helium droplets [26]. However, a strong interaction with the OCS core leads to localization of the  $\text{H}_2$  molecules [27] and pronounced anisotropy in rotational superfluid response [28]. Moreover, describing a small  $p\text{H}_2$  cluster as a liquid has many limitations because essentially all of its molecules reside on the surface.

The large, cold liquid clusters observed in this work provide a system that is much closer to the bulk phase, and thus particularly promising for the study of superfluidity in hydrogen. The size of the clusters in Fig. 3(e) can be obtained from the intensity of the surface band in Fig. 1. Taking into account that CARS intensity scales as square

of the number density [15], inversely proportional to the linewidth, and using the liquid drop model [29], the average size of the clusters was estimated to be  $N \approx 10^4$ . At higher  $X \geq 1\%$  the surface band could not be detected due to small fraction of the surface molecules in large clusters. Thus the size of the clusters in Figs. 3(a)–3(c) must be larger than  $2 \times 10^4$   $p\text{H}_2$  molecules.

The analysis of the rotational CARS spectra shows that the frequency jump of the  $Q_1(0)$  line of about  $1 \text{ cm}^{-1}$  in Fig. 2 is caused by the transition from solid to liquid clusters, at  $X \approx 1\%$ . Nevertheless, the  $Q_1(0)$  frequency for liquid clusters remains about  $1 \text{ cm}^{-1}$  lower than for bulk liquid at  $T = 18 \text{ K}$ . A similar spectral shift was observed in Ref. [11] where it was assigned to the effect of the lower temperature of the liquid  $p\text{H}_2$  clusters in the beam. Some additional shift may also be caused by the finite size effects in the clusters [11]. In comparison, the frequency of the  $S_0(0)$  line in Figs. 3(d) and 3(e) is found to be  $353.4 \text{ cm}^{-1}$ , which is nearly identical to the observed frequency of  $353.3 \text{ cm}^{-1}$  in bulk liquid at  $18 \text{ K}$  [17]. This is in agreement with the much smaller matrix shift of the  $S_0(0)$  line ( $\approx 1 \text{ cm}^{-1}$ ) as compared to that of the  $Q_1(0)$  line ( $\approx 10 \text{ cm}^{-1}$ ). Therefore the frequency of the  $S_0(0)$  line is expected to have about a factor of 10 smaller sensitivity to a change of the conditions in the clusters, such as higher density of the liquid at lower temperature [8].

We have prepared large  $p\text{H}_2$  clusters in a cryogenic pulsed nozzle beam expansion of neat and dilute  $p\text{H}_2$  in He and studied their aggregate states via CARS spectroscopy. We found that warm  $p\text{H}_2$  clusters are solid. On the other hand, clusters obtained from highly diluted  $p\text{H}_2$  gas remained liquid at  $T = 1\text{--}2 \text{ K}$ , which is in the range of the predicted superfluid transition temperature in  $p\text{H}_2$ . We conclude that clusters which first form and continue to grow at low temperature do not freeze and are expected to stay liquid down to  $T = 0 \text{ K}$  due to the low rate of both classical and quantum nucleation. In the future, we plan higher resolution measurements of the  $S_0(0)$  line in liquid clusters, which may give a spectroscopic probe for their superfluid state.

We are grateful to Professor Joseph Nibler for his help with setting up the CARS experiment and to Bobby Khalajestani and Russell Sliter for their help with some of the experiments described in this paper. This material is based upon work supported by the NSF under Grants No. CHE 0513163 and No. CHE 0432370.

---

\*Present address: Department of Chemistry, Massachusetts Institute of Technology, Cambridge, MA 02139, USA.

- [1] D.R. Tilley and J. Tilley, *Superfluidity and Superconductivity* (Institute of Physics Publ., Bristol and Philadelphia, 1990).  
 [2] W. Ketterle, in *Bose Einstein Condensates and Atom Lasers*, edited by S. Martellucci, A.N. Chester, A.

- Aspect, and M. Inguscio (Kluwer Academic, New York, 2000), p. 1.  
 [3] T. Legett, *Rev. Mod. Phys.* **71**, S318 (1999).  
 [4] V.L. Ginzburg and A. A. Sobyenin, *JETP Lett.* **15**, 242 (1972).  
 [5] S.M. Apenko, *Phys. Rev. B* **60**, 3052 (1999); V.S. Vorob'ev and S.P. Malysenko, *J. Phys. Condens. Matter* **12**, 5071 (2000).  
 [6] P. Sindzingre, D.M. Ceperley, and M.L. Klein, *Phys. Rev. Lett.* **67**, 1871 (1991); S. A. Khairallah, M.B. Sevryuk, D.M. Ceperley, and J.P. Toennies, *Phys. Rev. Lett.* **98**, 183401 (2007); F. Mezzacapo and M. Boninsegni, *Phys. Rev. Lett.* **100**, 145301 (2008).  
 [7] E. Cheng, M. A. McMahan, and K. B. Whaley, *J. Chem. Phys.* **104**, 2669 (1996).  
 [8] H. J. Maris, G. M. Seidel, and T. E. Huber, *J. Low Temp. Phys.* **51**, 471 (1983).  
 [9] H. J. Maris, G. M. Seidel, and F. I. B. Williams, *Phys. Rev. B* **36**, 6799 (1987).  
 [10] S. Goyal, D. L. Schutt, and G. Scoles, *J. Phys. Chem.* **97**, 2236 (1993).  
 [11] G. Tejeda, J. M. Fernandez, S. Montero, D. Blume, and J. P. Toennies, *Phys. Rev. Lett.* **92**, 223401 (2004).  
 [12] J. DeKinder, A. Bouwen, and D. Schoemaker, *Phys. Rev. B* **52**, 15 872 (1995); M. Schindler, A. Dertinger, Y. Kondo, and F. Pobell, *Phys. Rev. B* **53**, 11451 (1996).  
 [13] A. C. Clark, X. Lin, and M. H. W. Chan, *Phys. Rev. Lett.* **97**, 245301 (2006).  
 [14] M. N. Slipchenko, S. Kuma, T. Momose, and A. F. Vilesov, *Rev. Sci. Instrum.* **73**, 3600 (2002).  
 [15] R. D. Beck, M. F. Hineman, and J. W. Nibler, *J. Chem. Phys.* **92**, 7068 (1990).  
 [16] K. E. Kerr, T. Momose, D. P. Weliky, C. M. Gabrys, and T. Oka, *Phys. Rev. Lett.* **72**, 3957 (1994).  
 [17] S. S. Bhatnagar, E. A. Allen, and H. L. Welsh, *Can. J. Phys.* **40**, 9 (1962).  
 [18] G. Collins, W. G. Unites, E. R. Mapoles, and T. P. Bernat, *Phys. Rev. B* **53**, 102 (1996).  
 [19] J. van Kranendonk, *Solid Hydrogen. Theory of the Properties of Solid H<sub>2</sub>, HD and D<sub>2</sub>* (Plenum Press, New York and London, 1983).  
 [20] S. C. Durana and J. P. McTague, *Phys. Rev. Lett.* **31**, 990 (1973).  
 [21] D. R. Miller, in *Atomic and Molecular Beam Methods*, edited by G. Scoles (Oxford, New York, 1988), Vol. 1.  
 [22] S. Kuma, H. Goto, M. N. Slipchenko, A. F. Vilesov, A. Khramov, and T. Momose, *J. Chem. Phys.* **127**, 214301 (2007).  
 [23] M. Hartmann, R. E. Miller, J. P. Toennies, and A. Vilesov, *Phys. Rev. Lett.* **75**, 1566 (1995).  
 [24] E. L. Knuth, F. Schunemann, and J. P. Toennies, *J. Chem. Phys.* **102**, 6258 (1995).  
 [25] A. C. Levi and R. Mazzeo, *J. Low Temp. Phys.* **122**, 75 (2001).  
 [26] S. Grebenev, B. Sartakov, J. P. Toennies, and A. F. Vilesov, *Science* **289**, 1532 (2000).  
 [27] F. Paesani and K. B. Whaley, *J. Chem. Phys.* **124**, 234310 (2006).  
 [28] Y. Kwon and K. B. Whaley, *Phys. Rev. Lett.* **89**, 273401 (2002); Y. Kwon and K. B. Whaley, *J. Low Temp. Phys.* **134**, 269 (2004).  
 [29] J. Jortner, *Z. Phys. D* **24**, 247 (1992).